Antarctic Science 8 (2): 193–206 (1996)

Antarctic Peninsula granitoid petrogenesis: a case study from Mount Charity, north-eastern Palmer Land

JANE H. SCARROW, R.J. PANKHURST, P.T. LEAT and A.P.M. VAUGHAN

British Antarctic Survey, Natural Environment Research Council, High Cross, Madingley Road, Cambridge, CB3 0ET, UK

Abstract: At Mount Charity, north-eastern Palmer Land, Rb–Sr whole-rock dating has identified three successive phases of granitoid emplacement in Triassic (232 ± 4 Ma), Jurassic (168 ± 1 Ma), and Cretaceous (120 ± 4 Ma) times. The Triassic suite comprises tonalites, granodiorites (including one two-mica granodiorite), monzogranite and a granite having either I-type or S-like mineralogies. The Jurassic suite includes only S-like granites, and the Cretaceous biotite tonalites and biotite granodiorite are all I-type. The three suites have negative ∈Nd and positive ∈Sr, and have subtly different Nd and Sr isotope characteristics: Suite A, $\in Sr_t$ =+30 to +53 and $\in Nd_t$ =-0.9 to -3.1, Suite B, $\in Sr_t$ =+43 to +64 and $\in Nd_t$ =-2 to -5.3, Suite C, $\in Sr_t$ =+22 to +23 and $\in Nd_t$ =-2.5 to -2.6. Mineralogical and compositional differences between the three suites suggest that different sources were tapped. All the granitoids are isotopically intermediate in composition between Palmer Land crust and depleted asthenosphere. We suggest that the I-*type* granitoids were produced by melting of meta-igneous crust; by contrast, the S-*like* granitoids represent partial melts of garnet-bearing sedimentary crust. Syn-magmatic structures in Suite A are compared with known structural events in western Palmer Land and suggest that extension controlled Triassic pluton emplacement. The Jurassic magmas were also emplaced during an episode of arc extension, and intrusion of the Cretaceous magmas was probably controlled by regional extension and dextral transtension. Successive phases of magmatism focussed at Mount Charity are consistent with reactivated faults acting as magma conduits.

Received 2 June 1995, accepted 28 November 1995

Key words: geochronology, I-type granite, magmatic arc, petrogenesis, S-type granite

Introduction

The Antarctic Peninsula magmatic arc is an extension of the Andean orogenic belt and is related to eastward subduction of oceanic lithosphere (Suárez 1976, Saunders & Tarney 1982, Pankhurst 1982, 1990). The exposed arc is partly plutonic, and partly volcanic. The plutonic rocks range in age from Middle Triassic to Tertiary (Rex 1976, Pankhurst 1982, Leat *et al.* 1995), and are mafic–silicic, calc-alkaline, and dominated by diorite, granodiorite, and granite. Previous work (Saunders *et al.* 1980, Pankhurst 1982, 1990, Pankhurst *et al.* 1988, Hole *et al.* 1991) established that the plutonic rocks of Graham Land form approximately coast-parallel belts showing two secular trends in space and time:

a) plutonism migrated westward (trench-ward) between Triassic and Tertiary times,

b) $^{87}Sr/^{86}Sr_i$ decreased at the same time, with corresponding increases in $^{143}Nd/^{144}Nd_i$.

Pankhurst (1982) suggested that these trends represented decreasing crustal involvement as the zone of magma generation migrated westward away from the margin of the pre-existing continent. Pankhurst *et al.* (1988) explained these relationships in terms of changing subduction regime, whereby the slab steepened as it rolled back, generating progressively deeper sourced magmas. Additional geochemical data were used by Hole *et al.* (1991) to classify the main magma types within what appeared to be a mixing series, and to suggest that relatively uncontaminated mantle-derived magmas had a progressively easier passage through the crust as the arc evolved. The degree to which these secular variations in magma compositions were controlled by lateral variations in crustal composition independently of time is unclear. As magmatism migrated westward, the melts could have intruded into, or derived from, progressively younger, less differentiated crust. Localized variations in crustal sources or contaminants might have produced local variations in magma composition (Hole *et al.* 1991). Nevertheless, Storey & Alabaster (1991) proposed that the Sr and Nd isotopic compositions of eastern Antarctic Peninsula granitoids might have been inherited from enriched lithospheric mantle sources. Early Jurassic plutons in north-eastern Palmer Land are of two extreme types (Wever *et al.* 1994, 1995):

a) leucocratic granites with high $^{87}Sr/^{86}Sr_i$ that contain large contributions from partial melts of local metasedimentary crustal sources

b) low $^{87}Sr/^{86}Sr_i$ I-type granodiorites that were emplaced in the same general area and at the same time.

By contrast, crustal involvement in Antarctic Peninsula plutonism of Cretaceous age is much more difficult to establish. Cretaceous plutons are widely distributed in northern Palmer Land, and constitute the only plutonic group recognized in southern Palmer Land. Pankhurst & Rowley (1991) suggested derivation of the latter by fractional crystallization of mantle-derived magmas, with localized assimilation of crust, whereas Leat *et al.* (1995) proposed that the main suite of Cretaceous granitoids throughout the Antarctic Peninsula was derived by partial melting of igneous lower crust.

This paper uses new geochronological, petrographic, and compositional data from Mount Charity in north-eastern Palmer Land to test some of the above models. New Rb–Sr whole-rock data for granitoids from the small (400 km^2) area identify three phases of plutonism in Triassic, Jurassic, and Cretaceous times. This eliminates the space variable as a control on magma-composition, so enabling isolation of the effects of different tectonic regimes and magma plumbing systems at three different times.

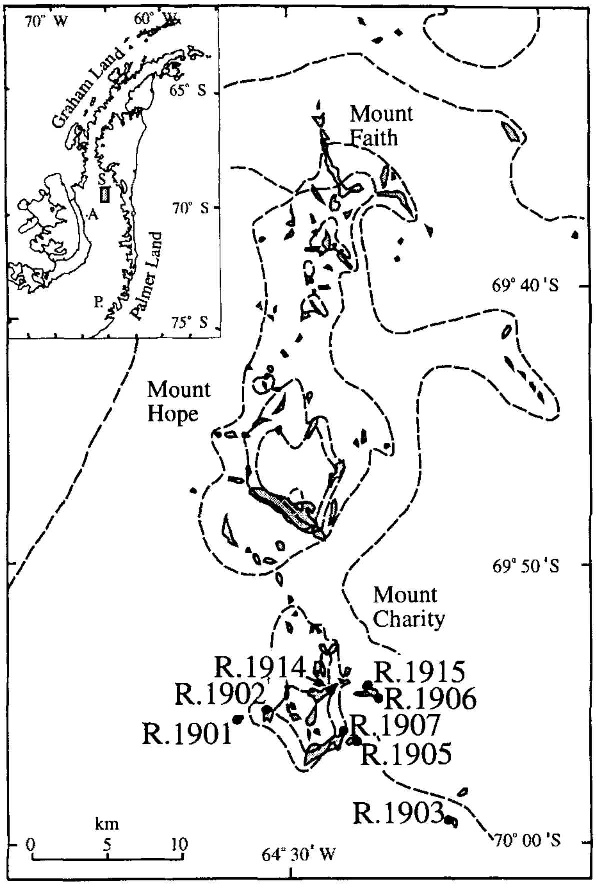

Fig. 1. Sketch maps showing the location of Mount Charity in the Eternity Range. Inset shows Antarctic Peninsula, shaded block is the area covered by Eternity Range map. Shaded areas in main map represent rock outcrops. S = Mount Sullivan, A = Auriga Nunataks, P = Mount Poster.

Geology of the Mount Charity area

The Eternity Range is a north–south mountain chain, 45 km long by 13 km wide, comprising Mount Faith (2650 m), Mount Hope (2862 m), and Mount Charity (2680 m) (Fig. 1). Mount Charity has three peaks within 100 m altitude of each other, rising from the surrounding 2000 m plateau as 500 m-high ridges separated by wide, gently sloping cirques. The eastern faces are the steepest and the main rock exposures are on the southern side of the mountain. Although several geologists have visited the mountain, the geology is not well known because of poor accessibility and complex relationships between the plutonic rocks. Early work established that pink granites comprise the bulk of the massif (Davies 1971, 1984). Pankhurst (1981) visited all readily accessible exposures of the Mount Charity granite complex on the east, west, and south–east sides of the mountain, and found a greater variety of rock types than described by Davies.

High on the main eastern summit ridge of the mountain, poorly sorted, poorly consolidated sandstones, siltstones, and conglomerates overlie the plutonic rocks (Davies 1984). The sedimentary rocks, estimated to have a maximum thickness of 650 m (Davies 1984), are of local origin, containing clasts of many of the regional igneous rock types and including rounded boulders up to 1 m in diameter. Wind-faceted pebbles are present in arkosic sandstones and siltstones which indicates that components of the deposits had been modified by sub-aerial processes. Also present are clasts of gneissose granite and undeformed volcanic rocks (ignimbrites). The main granitoids are the abundant leucocratic granite that appears to constitute the mass of the summit, and a coarser-grained alkali-feldspar porphyritic granite. They are generally free of mafic inclusions. Farther along the eastern extension of this long ridge, the pink granites are accompanied by more mafic granodiorite or diorite which exhibits a characteristic rusty weathering. Contacts between these rock types were not observed.

On the western ridges a pink, medium-grained, equigranular, biotite–hornblende granite crops out. There, steeply dipping dolerite dykes (1–3 m wide) cause a disproportionate darkening of the screes. A similar, but slightly foliated, granite, containing two 3 m inclusions of amphibolite, crops out 5 km south of Mount Charity.

The south-eastern exposures display considerable complexity (Fig. 2), with at least six different rock types. They have a chaotic intrusive structure, with the apparent order of intrusion being:

a) Weakly foliated, medium- to coarse-grained hornblende *diorite* (Fig. 2) containing minor biotite as large masses within other intrusive rocks and itself containing small amphibolite xenoliths. The xenoliths locally contain pink feldspar megacrysts which also occur in the diorite, where deformed xenoliths are schistose and disrupted as schlieren.

b) A coarsely porphyritic *granodiorite/granite*, with pink alkali feldspar phenocrysts up to 3 cm long, intruding the diorite.

c) *Leucocratic granite* (Fig. 2), with a characteristic aplitic texture as the most abundant rock type. It intrudes all the above as an amorphous mass and as discrete sheets. It varies from light brown-pink and massive, to grey with streaky bands of amphibole close to enclaves and xenoliths of amphibolitic diorite. Its grain size varies from fine, to medium with druses of quartz and muscovite.

d) Feldspar *porphyry* with a fine-grained grey matrix. The matrix colour grades to black at its contact with the leucocratic granite, due to either chilling or shearing.

e) Coarse muscovite *pegmatite* (Fig. 2), which in some places grades into the leucocratic granite and in others cuts it as discrete bands.

f) *Dolerite dykes*, with sparse, 0.3 cm, stubby hornblende phenocrysts, forming two conjugate sets trending 110° and 200°.

We interpret this sequence as an intermediate-to-acid complex, with the main phase being the Mount Charity leucocratic granite (c).

Petrography

The granitoids grade temporally from medium- (1–5 mm) to fine- (<1 mm) grained and have subhedral, equigranular textures. They may be divided into three suites. Suite A comprises tonalites, granodiorites (including one two-mica granodiorite), monzogranites, and a granite. Suites B and C have more restricted compositions, the former comprising granites, and the latter a biotite granodiorite and biotite tonalites.

All the suites contain plagioclase, alkali feldspar, biotite, quartz, and magnetite, in proportions that vary with composition, and chlorite, epidote, and pyrite, of probable hydrothermal origin. Suite A is characterized by magnesio-hornblende, muscovite (primary and secondary), apatite, titanite, and zircon in varying amounts. Fe–Ti oxides are sparse. Post-crystallization strain is common in this suite as indicated by strained quartz and myrmekite (the latter being a strain-enhanced replacement texture; Simpson & Wintsch 1989). Suite B contains muscovite (primary and secondary) and ilmenite. In addition, perthitic and anti-perthitic textures in the feldspars, and a paucity of mafic minerals also serve to distinguish this suite petrographically. Suite C has a diverse mineralogy comprising varying amounts of magnesio-hornblende, edenite, diopside, augite, hypersthene, apatite, titanite, and zircon. The plagioclase feldspars from this suite are typically zoned and Fe–Ti oxides are abundant. Table I presents representative mineral analyses from samples from each of the suites. Full compositional datasets may be obtained on application to the Head of Geoscience Division, British Antarctic Survey.

The cores of fresh feldspar phenocrysts have variable compositions (Table I). Suite C apparently has the most systematic variation (Fig. 3): both Suite C samples have distinct plagioclase and alkali feldspar populations, with one sample (R.1906.5) generally having plagioclases with higher albite concentrations and alkali feldspars with higher orthoclase concentrations than the other (R.1906.7). The higher Ab and Or components correspond to the higher whole-rock SiO_2 (Table II), and the analysed feldspars are plausibly equilibrium phenocryst compositions related to magmatic evolution by fractional crystallization. Suite C plagioclases are strongly oscillatory-zoned, probably as a result of rapid, shallow-level crystallization without time for magma–crystal equilibration (Pitcher 1993).

Fig. 2. Cross-cutting relationships at Mount Charity, station R.1907. Diagonal sheet of pegmatite (left of lens cap) cutting leucogranite (left foreground) that intrudes diorite (right foreground). Lens cap is 5 cm in diameter.

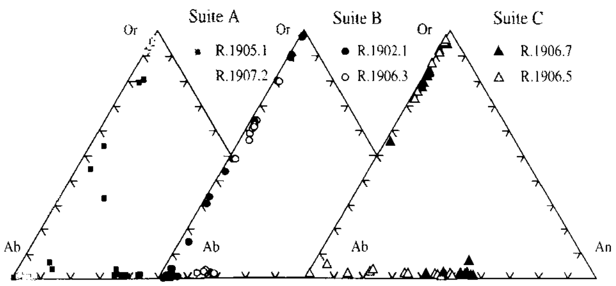

Fig. 3. Feldspar compositions from the three suites of granitoids, Mount Charity, plotted in Or–Ab–An diagrams. Feldspar compositions measured by electron microprobe, details of which are given at the base of Table I.

https://doi.org/10.1017/S0954102096000260 Published online by Cambridge University Press

Table I. Representative mineral analyses for Mount Charity samples.

	Suite A									Suite B			
	Pl		Af		Bt	Ms	Amp	Ap	Mag	Pl		Af	Bt
	R.1905.1	R.1907.2	R.1905.1	R.1907.2	R.1905.1	R.1907.2	R.1905.1	R.1905.1	R.1905.1	R.1902.1	R.1906.3	R.1906.3	R.1906.3
SiO_2	58.67	68.10	63.16	65.25	37.19	45.06	45.69	0.30	0.26	67.82	65.51	66.68	24.81
TiO_2	0.04	0.03	0.23	-	3.02	0.38	0.88	0.06	0.10	0.00	-	0.11	0.20
Al_2O_3	26.16	20.01	22.08	18.35	14.57	27.78	9.10	-	1.45	20.26	22.36	19.29	20.05
Cr_2O_3	0.07	0.01	-	-	0.13	-	0.10	0.02	8.62	0.03	-	0.02	0.01
FeO	-	-	-	-	17.92	6.19	16.65	0.32	60.25	-	-	-	31.33
Fe_2O_3	0.15	0.07	0.09	-	-	-	-	-	28.98	0.10	0.08	0.01	-
MnO	-	-	0.01	0.06	0.34	0.22	0.45	-	0.88	-	0.05	-	0.67
MgO	-	0.00	0.02	0.04	13.20	2.39	11.83	0.03	0.11	-	0.05	0.05	11.73
CaO	8.13	0.83	3.22	0.09	0.03	0.13	12.29	56.21	0.30	0.38	2.99	0.22	0.05
Na_2O	7.00	10.89	6.07	0.73	0.39	0.14	1.13	0.12	0.34	11.30	8.89	4.17	0.35
K_2O	0.12	0.05	5.68	16.28	9.84	10.56	0.88	0.04	-	0.38	0.54	10.40	0.03
SO_2	-	-	0.07	0.04	0.09	0.06	0.07	0.04	0.03	-	0.03	-	-
P_2O_5	-	0.11	0.04	0.10	-	0.04	0.05	42.90	0.05	0.17	0.07	0.08	-
Total	100.30	99.93	100.45	100.76	96.73	92.70	98.98	99.95	101.38	100.45	100.30	100.89	89.34
Si	2.61	2.97	2.82	2.99	5.58	6.36	6.74	0.05	0.01	2.96	2.87	2.98	3.82
Al IV	1.37	1.03	1.16	0.99	2.42	1.63	1.30	-	0.07	1.04	1.15	1.02	3.63
Al VI					0.16	2.98	0.28						
Ti	0.00	0.00	0.01	-	0.34	0.04	0.10	0.01	0.00	0.00	-	0.00	0.02
Cr	0.00	0.00	-	-	0.02	-	0.01	0.00	0.28	0.00	-	0.00	0.00
Fe II	-	-	-	-	2.25	0.73	2.05	0.05	2.05	-	-	-	4.03
Fe III	0.01	0.00	0.00	-	-	0.00	-	-	0.89	0.00	0.00	0.00	-
Mn	-	-	0.00	0.00	0.04	0.03	0.06	-	0.03	-	0.00	-	0.09
Mg	-	0.00	0.00	0.00	2.95	0.50	2.60	0.01	0.01	-	0.00	0.00	2.69
Ca	0.39	0.04	0.15	0.00	0.01	0.02	1.94	10.28	0.01	0.02	0.14	0.01	0.01
Na	0.61	0.92	0.53	0.06	0.11	0.04	0.32	0.04	0.03	0.96	0.75	0.36	0.10
K	0.01	0.00	0.32	0.95	1.88	1.90	0.16	0.01	-	0.02	0.03	0.59	0.01
S	-	-	0.00	0.00	0.01	0.01	0.01	0.01	0.00	-	0.00	-	-
P	-	0.00	0.00	0.00	0.00	0.01	0.01	6.20	0.00	0.01	0.00	0.00	-

All three groups contain quartz.
Analyses made on the Cameca SX50 microprobe facility at the University of Cambridge, UK, using standard operating conditions (accelerating voltage 20 kV, beam current 10 nA, ED AN10000 analysis, software ZAF4).

Suite A has a broadly similar distribution of feldspar compositions to that of Suite C. Granite R.1907.2 contains only Ab-rich plagioclases and Or-rich alkali feldspars, indicating likely equilibrium compositions. The more mafic Suite A sample, R.1905.1, has alkali feldspar compositions that are consistent with equilibrium during fractional crystallization in a single-liquid line of descent. Nevertheless, plagioclase compositions of R.1905.1 are bimodal with a main Ab-poor cluster (An_{34}–An_{43}), and a minor, Ab-rich one (An_1–An_{10}). This distribution cannot represent equilibrium with a single liquid, and plausibly resulted from mingling of a silicic magma containing albite with the mafic magma containing Ab-poor phenocrysts.

By contrast, Suite B alkali feldspars are compositionally diverse, covering the range Or_{13}–Or_{98}, with weak clustering. This distribution of compositions is unlikely to have resulted from equilibrium growth in any magma composition, or in a series of compositions related by fractional crystallization. More likely, the feldspars represent xenocrysts derived from partial assimilation of several protoliths, and/or from mingling of several magmas.

There are significant differences in ferromagnesian mineralogy between the suites. The mineralogy of suites A and C indicates relatively oxidized crystallization conditions, whereas that of Suite B suggests more reduced conditions. The presence of magnesio-hornblende in the granitoids from suites A and C indicates substitution of Mg^{2+} for Fe^{2+}, and hence a high Fe^{3+}/Fe^{2+} (i.e. a high fO_2) melt (Czamnske *et al.* 1981). The presence of titanite also indicates fO_2 above the QFM buffer (Carmichael & Nicholls 1967). In addition, co-precipitation of hornblende and biotite indicates that water activity caused deviation from the expected order of crystallisation, i.e. hornblende followed by biotite. In contrast, Suite B contains no amphibole, and has, in common with some samples of Suite A, two micas. The dominance of ilmenite over magnetite in Suite B, resulted from lower fO_2.

https://doi.org/10.1017/S0954102096000260 Published online by Cambridge University Press

Table I continued.

	Suite B		Suite C										
	Ilm	Mag	Pl		Af	Bt	Amp		Opx	Cpx		Ap	Mag
	R.1906.3	R.1906.3	R.1906.5	R.1906.7	R.1906.7	R.1906.5	R.1906.5	R.1906.7	R.1906.5	R.1906.5	R.1906.7	R.1906.7	R.1906.7
SiO_2	0.17	0.34	59.52	54.63	65.22	36.39	47.62	43.36	51.36	51.00	52.29	0.22	0.22
TiO_2	47.40	1.79	0.02	-	0.08	4.58	1.05	0.07	0.26	0.39	0.30	0.01	2.73
Al_2O_3	-	0.45	25.65	28.45	18.68	12.93	5.75	7.54	1.90	3.16	1.10	-	0.64
Cr_2O_3	-	0.02	0.02	-	0.02	0.04	0.02	0.01	0.04	0.06	0.06	-	0.42
FeO	33.91	65.36	-	-	-	21.27	17.85	18.83	25.58	16.64	11.34	0.48	62.59
Fe_2O_3	11.79	33.05	0.22	0.35	0.14	-	-	-	-	-	-	-	33.53
MnO	8.62	0.48	-	0.01	-	0.29	0.65	0.53	0.56	0.77	0.42	-	0.26
MgO	0.00	-	-	0.02	-	11.39	12.14	15.50	19.50	13.75	13.44	0.04	0.03
CaO	0.13	0.04	7.29	10.82	0.14	0.01	11.34	7.88	1.60	11.13	21.81	54.42	0.06
Na_2O	0.05	0.21	7.51	5.31	2.37	0.15	1.39	0.22	0.17	0.98	0.36	-	0.39
K_2O	0.03	0.04	0.41	0.32	13.61	9.36	0.65	0.10	-	0.33	-	0.03	0.01
SO_2	-	-	-	0.05	0.02	0.09	0.05	-	0.01	0.08	0.03	0.31	-
P_2O_5	-	-	0.17	0.09	0.11	0.05	0.15	0.07	0.07	0.12	0.16	42.17	0.13
Total	102.10	101.80	100.79	99.87	100.22	96.31	98.58	93.97	100.79	98.16	101.53	97.94	101.03
Si	0.00	0.01	2.64	2.47	2.98	5.56	7.07	6.73	1.93	1.95	1.95	0.04	0.01
Al IV	-	0.02	1.34	1.52	1.01	2.33	0.93	1.27	0.08	0.14	0.05	-	0.03
Al VI							0.08	0.11					
Ti	0.89	0.06	0.00	-	0.00	0.53	0.12	0.01	0.01	0.01	0.01	0.00	0.08
Cr	-	0.00	0.00	-	0.00	0.01	0.00	0.00	0.00	0.00	0.00	-	0.01
Fe II	0.70	2.26	-	-	-	2.72	2.22	2.44	0.80	0.53	0.35	0.07	2.15
Fe III	0.22	1.03	0.01	0.01	0.00	-	-	-	-	-	-	-	1.04
Mn	0.18	0.02	-	0.00	-	0.04	0.08	0.07	0.02	0.03	0.01	-	0.01
Mg	0.00	-	-	0.00	-	2.59	2.69	3.58	1.09	0.78	0.74	0.01	0.00
Ca	0.00	0.00	0.35	0.52	0.01	0.00	1.80	1.31	0.06	0.46	0.87	10.17	0.00
Na	0.00	0.02	0.65	0.47	0.21	0.04	0.40	0.06	0.01	0.07	0.03	-	0.03
K	0.00	0.00	0.02	0.02	0.79	1.82	0.12	0.00	-	0.02	-	0.01	0.00
S	-	-	-	0.00	0.00	0.01	0.01	-	0.00	0.00	0.00	0.05	-
P	-	-	0.01	0.00	0.00	0.01	0.02	0.01	0.00	0.00	0.00	6.23	0.00

Mineral abbreviations: Pl, plagioclase; Af, alkali feldspar; Bt, biotite; Ms, muscovite; Amp, amphibole; Ap, apatite; Mag, magnetite; Ilm, ilmentite; Opx, orthopyroxene; Cpx, clinopyroxene. Number of oxygens in structural formulae; feldspar, 8; mica, 20, anhydrous; amphibole, 22, anhydrous; pyroxene, 6; apatite, 26. Fe oxides recalculated using the equations of Carmichael & Nicholls (1967); Mag=4 Os, Ilm=3 Os.

Moyes (1991) suggested that an eastward decrease in fO_2 of Antarctic Peninsula granitoid magmas resulted from crystallization of more reduced magmas at increasing distance from the trench. However, it is more likely that fO_2 was controlled by source characteristics.

The petrographic features of the suites are compared with published criteria for the discrimination of I-type and S-type granites (Beckinsale 1979, Chappell & White 1992, Pitcher 1993, p. 111) for classification purposes. None of the rocks satisfy criteria of S-type granites, but many show trends towards such compositions and so, in this paper, we refer to them as S-*like*. Suite A granitoids are divisible into those having peraluminous (broadly S-*like*) and metaluminous (broadly I-type) mineralogy. The S-like varieties are the SiO_2-rich rocks and the I-type ones are relatively mafic. The suite as a whole has an intermediate position with regard to S- and I-type classification. Suite B granitoids have the most peraluminous mineralogy, e.g. no hornblende, and are strongly reduced, containing ilmenite. They are distinctly S-like, and equivalent to the "modified I-types" of Graham Land (Pankhurst 1990). Suite C granitoids have metaluminous mineralogy, they contain biotite and hornblende, and are I-type.

Geochronology

Rb–Sr whole-rock dating was used to investigate the crystallization history of the Mount Charity granitoids, for which no previous geochronological or isotopic data exist. Analyses were carried out on a fully-automated 5-collector VG 354 mass-spectrometer at the Isotope Geology Unit of the British Geological Survey in London (now NERC Isotope Geosciences Laboratory, Keyworth) using the method employed by Pankhurst & Rowley (1991). Some samples were re-analysed more recently on a MAT 262 multi-collector machine at Keyworth and show good agreement with the

Table II. Representative whole-rock compositions of Mount Charity samples.

	Suite A						Suite B					Suite C		
Sample	R.1905.1	R.1905.2	R.1905.4	R.1905.5	R.1905.8	R.1907.2	R.1906.3	R.1902.1	R.1907.4	R.1914.11	R.1915.1	R.1906.2	R.1906.5	R.1906.7
SiO_2	55.67	60.93	71.59	75.28	54.85	75.07	77.24	76.76	77.16	68.76	76.93	71.34	65.89	57.56
TiO_2	0.81	0.84	0.23	0.07	0.75	0.06	0.13	0.06	0.06	0.38	0.14	0.28	0.53	0.79
Al_2O_3	17.59	16.62	14.71	13.73	16.98	14.16	12.56	12.39	12.38	16.22	12.25	14.08	15.22	16.43
Fe_2O_3T	7.13	5.88	2.35	0.49	8.21	0.48	1.29	0.97	1.09	2.73	1.25	2.6	4.88	8.37
MnO	0.13	0.12	0.03	0.02	0.17	0.02	0.02	0.04	0.03	0.04	0.02	0.05	0.08	0.14
MgO	4.64	2.61	0.49	0.02	5.17	0.09	0.01	0	0	1.1	0.02	0.69	1.66	3.86
CaO	6.32	4.86	1.53	0.68	6.73	0.75	0.48	0.36	0.51	3.01	0.64	2.08	3.59	6.57
Na_2O	3.26	3.38	3.12	4.1	3.17	4.28	3.6	4.15	3.71	3.84	3.32	3.1	3	2.75
K_2O	2.3	2.96	5.51	4.34	2.29	4.91	4.67	4.32	4.88	2.84	4.74	4.8	4.1	2.33
P_2O_5	0.38	0.26	0.07	0.04	0.38	0.02	0	0	0	0.15	0	0.05	0.12	0.16
LOI	1.64	1.3	0.84	0.84	1.56	0.5	0.33	0.68	0.58	1.17	0.66	0.66	0.56	1.35
Total	99.87	99.75	100.46	99.59	100.26	100.36	100.32	99.72	100.39	100.23	99.96	99.73	99.63	100.31
Ba	499	681	1169	260	347	94	894	33	72	736	975	479	659	498
La	24	27	82	4	19	7	25	6	6	27	22	27	33	24
Ce	62	75	142	15	45	21	54	36	47	75	43	45	78	59
Nd	35	26	38	10	28	10	31	27	34	35	21	20	22	31
Cl	84	74	29	22	62	24	6	18	24	37	40	77	508	281
S	95	59	58	59	61	71	70	58	57	57	57	60	63	64
Cr	149	19	6	2	195	3	1	1	2	3	1	5	12	24
Cu	12	13	14	0	15	5	1	0	1	6	3	13	34	44
Ga	28	23	15	19	31	21	15	19	19	25	14	14	15	18
Nb	12	11	5	10	16	13	11	17	20	6	7	16	14	9
Ni	58	10	2	1	64	0	0	0	1	2	1	3	9	20
Pb	17	26	42	62	24	41	30	32	17	22	22	35	29	22
Rb	153	153	185	251	140	249	196	212	236	112	189	305	241	119
Sr	776	531	491	122	622	117	69	29	51	663	77	165	228	319
Th	6	27	33	0	9	4	16	21	26	7	11	39	27	14
V	163	130	41	3	177	14	22	5	4	63	7	47	98	191
Y	31	29	11	8	57	17	38	44	53	13	20	38	39	32
Zn	107	82	30	32	120	19	33	43	29	50	27	32	59	76
Zr	154	141	179	39	143	32	131	112	119	149	109	154	226	151

older data (see Table III). For consistency, all the isochron fits were calculated using the earlier analyses, but with error estimates on the $^{87}Sr/^{86}Sr$ ratios increased to 0.015% (1-σ) compared with the value of 0.01% assumed for more recent data. The 30 analyses listed in Table III conform to three distinct isochrons which are interpreted as defining three separate igneous suites (Fig. 4).

a) Suite A. This consists of all but one of the samples from south-eastern Mount Charity (stations R.1905 and R.1907). Nine of these samples gave an errorchron (MSWD=4.2) which yielded an age of 232 ± 4 Ma (Middle–Late Triassic), with an initial $^{87}Sr/^{86}Sr$ of 0.7066 ± 0.0002. Although the distribution of the data is not continuous, essentially the same age and error are obtained if the high Rb/Sr leucocratic granite R.1905.6 is omitted. Three of the remaining four samples from these stations, a foliated diorite (R.1905.3), a pegmatite (R.1905.7) and an aplite (R.1905.9) fall close to this line, but increase the scatter unacceptably (MSWD= 20); the fourth, the chilled K-feldspar porphyry R.1907.4 appears to belong to Suite B.

b) Suite B. Fourteen samples with an even spread of Rb/Sr ratios define an isochron (MSWD= 2.7) corresponding to an age of 168 ± 1 Ma (Middle Jurassic). This suite includes all the leucocratic granites from stations R.1901(.2), R.1902 (.1, .2), R.1903 (.1, .2), R.1906 (.3, .4), R.1914 (.9) and R.1915 (.1, .2), representing the principle granite mass of Mount Charity, as well as the porphyritic granites from R.1914 (.10, .11) and the porphyry at R.1907 (.4) and the granite exposed at the nunatak 5 km south of Mount Charity, R.1903 (.1, .2, .3). The initial $^{87}Sr/^{86}Sr$ of 0.7080 ± 0.0001 is significantly higher than that of Suite A.

c) Suite C. Four samples from station R.1906 (.2, .5, .6, .7), of the rusty-weathering granodiorite, lie on a perfect isochron (MSWD= 0.1) which gives an age of 120 ± 4 Ma (Early Cretaceous), with an initial $^{87}Sr/^{86}Sr$ of 0.7059 ± 0.0002.

These three ages fit well with Triassic, Jurassic and Early

https://doi.org/10.1017/S0954102096000260 Published online by Cambridge University Press

Table III. Rb–Sr and Sm–Nd isotopic data for Mount Charity samples. (Sr (MAT) refers to recent repeat analyses of the samples).

	Age (Ma)	Rb (ppm)	Sr (ppm)	$^{87}Rb/^{86}Sr$	S.D.	$^{87}Sr/^{86}Sr$	Sr (MAT)	$\in(Sr)_t$	Sm	Nd	$^{147}Sm/^{144}Nd$	$^{143}Nd/^{144}Nd$	$^{143}Nd/^{144}Ndi$	$\in(Nd)_t$
R.1905.1	232±4	150	770	0.5628	0.5	0.70834	0.708310	31.99	7.656	35.462	0.1305	0.512381	0.512182	-3.1
R.1905.2	232±4	150	526	0.8268	0.5	0.70923	-	32.21	-	-	-	-	-	-
R.1905.3	232±4	112	573	0.5637	0.5	0.70921	-	44.3	-	-	-	-	-	-
R.1905.4	232±4	185	489	1.0911	0.5	0.71031	0.710342	35.1	6.252	49.266	0.0767	0.512298	0.512181	-3.1
R.1905.5	232±4	245	117	6.0764	0.5	0.72656	0.726105	31.25	1.17	3.933	0.1799	0.51257	0.512296	-0.9
R.1905.6	232±4	437	22	57.5911	1.1	0.89279	-	-32.57	-	-	-	-	-	-
R.1905.7	232±4	542	37	42.8091	0.8	0.84197	-	-58.57	-	-	-	-	-	-
R.1905.8	232±4	137	610	0.6464	0.5	0.70873	-	33.59	-	-	-	-	-	-
R.1905.9	232±4	240	334	2.0857	0.5	0.71484	-	52.62	-	-	-	-	-	-
R.1907.1	232±4	220	78	8.2106	0.5	0.73432	-	41	-	-	-	-	-	-
R.1907.2	232±4	242	113	6.2259	0.5	0.72698	0.726947	30.17	1.597	4.563	0.2116	0.512503	0.51218	-3.1
R.1907.3	232±4	146	626	0.6735	0.5	0.70915	-	38.28	-	-	-	-	-	-
R.1901.2	168±1	200	25	23.3101	1.1	-	0.764350	57.4	-	-	-	-	-	-
R.1902.1	168±1	208	26	23.6949	1.0	0.76434	-	44.16	-	-	-	-	-	-
R.1902.2	168±1	148	484	0.8842	0.6	0.71036	-	55.9	-	-	-	-	-	-
R.1903.1	168±1	165	99	4.8326	0.5	-	0.719380	49.3	-	-	-	-	-	-
R.1903.2	168±1	107	830	0.3727	0.5	-	0.708652	49.1	-	-	-	-	-	-
R.1903.4	168±1	275	29	27.9355	0.9	0.77594	-	64.2	-	-	-	-	-	-
R.1906.3	168±1	190	65	8.504	0.5	0.72844	0.728471	52.67	5.677	25.158	0.1364	0.512401	0.51225	-3.4
R.1906.4	168±1	183	49	10.6844	0.5	0.73379	-	54.24	-	-	-	-	-	-
R.1907.4	168±1	231	48	13.9566	0.5	0.74089	0.740758	43.42	6.896	23.696	0.1759	0.512516	0.512321	-2
R.1914.9	168±1	213	32	19.1422	0.9	0.75352	-	45.58	-	-	-	-	-	-
R.1914.10	168±1	110	674	0.4745	0.5	0.70896	-	50	-	-	-	-	-	-
R.1914.11	168±1	110	659	0.4852	0.5	0.70923	0.709047	53.47	5.246	31.042	0.1022	0.512262	0.512149	-5.3
R.1915.1	168±1	183	73	7.3078	0.5	0.72549	-	51.59	-	-	-	-	-	-
R.1915.2	168±1	171	68	7.3565	0.6	0.72551	-	50.21	-	-	-	-	-	-
R.1906.2	120±4	297	158	5.4372	0.5	0.7152	-	22.29	-	-	-	-	-	-
R.1906.5	120±4	233	219	3.0858	0.5	0.71117	0.711119	22.01	6.656	34.147	0.1178	0.512452	0.512359	-2.5
R.1906.6	120±4	132	320	1.1939	0.5	0.70798	-	22.53	-	-	-	-	-	-
R.1906.7	120±4	114	312	1.0612	0.5	0.70773	0.707726	22.19	5.202	17.685	0.1778	0.512492	0.512352	-2.6

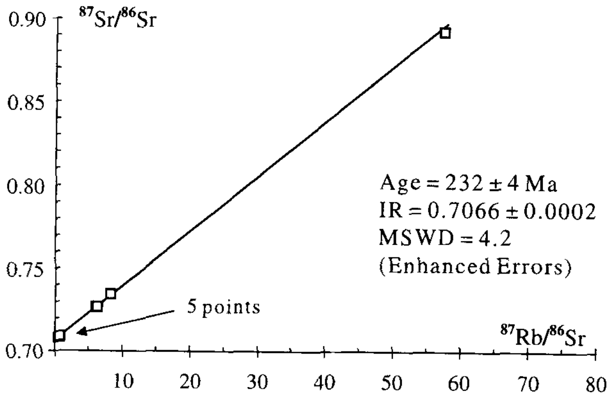

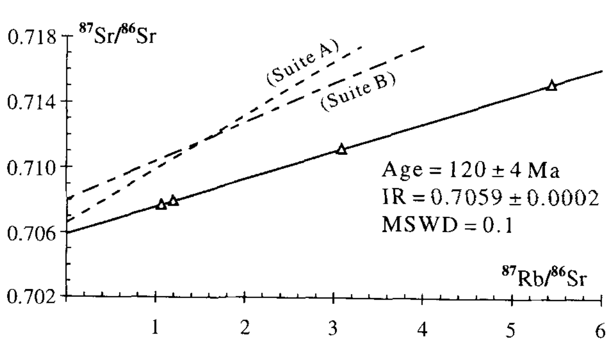

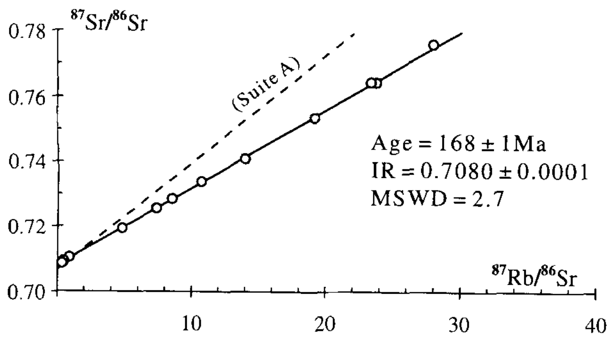

Fig. 4. Rb–Sr whole-rock isochron diagrams for the three suites of granitoids at Mount Charity.

https://doi.org/10.1017/S0954102096000260 Published online by Cambridge University Press

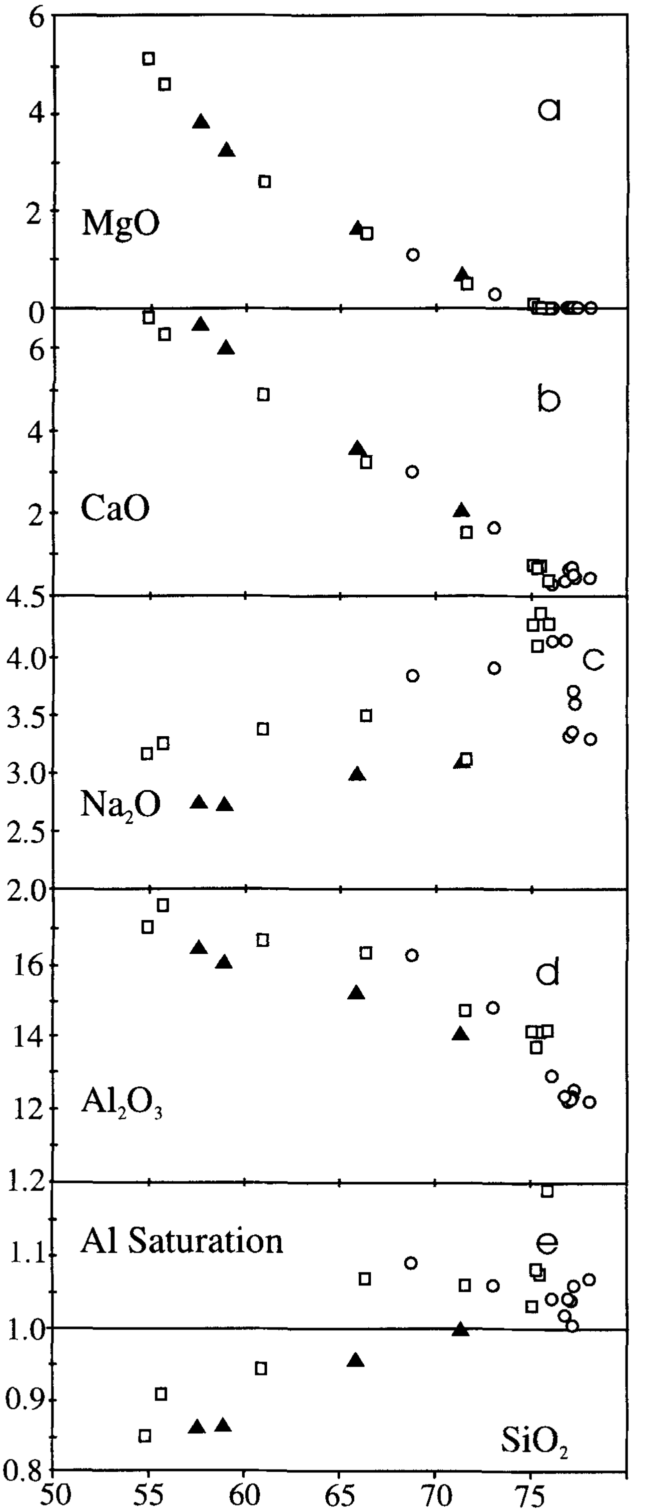

Fig. 5. Harker diagrams for selected major element whole-rock compositions of the three suites of granitoids, Mount Charity. Symbols:□ = Suite A, ○ = Suite B, ▲ = Suite C. Al saturation is molecular Al/(Ca+Na+K).

Cretaceous times of plutonism recognized elsewhere in the Antarctic Peninsula (Leat *et al.* 1995), and it is considered that each represents a distinct intrusive episode. There are few places in the Antarctic Peninsula where successive emplacement of Triassic, Jurassic and Early Cretaceous plutons has been recognized; the phenomenon is only known from northern Palmer Land, and Mount Charity is the only such location for which we have compositional data sets. This successive plutonism in a single spot eliminates the space variable in the secular trends of Antarctic Peninsula magmatism, and offers the opportunity to study differences in magma compositions at different times in the same crustal volume. Potentially, different sources tapped during the different magmatic episodes may relate to changing subduction regime (Pankhurst *et al.* 1988). The observed increase in $^{87}Sr/^{86}Sr$ between 232 ± 4 Ma (Suite A) and 168 ± 1 Ma (Suite B) can be explained by uniform growth of radiogenic Sr in a reservoir with an Rb/Sr ratio of 0.2–0.3, possibly an indication of a common crustal source region. The lower $^{87}Sr/^{86}Sr$= 0.7059 in Suite C granitoids is strong evidence for a different source, as well as ruling out crystallization of these rocks during one of the earlier events with resetting in Cretaceous times. The composition of the granitoids was therefore investigated to clarify the petrogenetic history.

Geochemistry

Major and trace elements

Major and trace element abundances were determined by standard XRF methods at the University of Keele, UK (Floyd 1985); representative data are presented in Table II. Selected major element variations are shown on Harker diagrams in Fig. 5. All the Mount Charity granitoids are calc-alkaline. The three suites have different silica distributions: suites A and C have fairly large ranges in SiO_2 (54.8–75.9 and 57.6–71.3 wt.% respectively) whereas Suite B has a more restricted range (68.8–78.1) and is more uniformly SiO_2-rich. Suites A and C have representatives with relatively high MgO and CaO abundances, up to approximately 5 wt.% and 7 wt.% respectively (Fig. 5a, b), and display smooth decreases in MgO and CaO with increasing SiO_2. These relationships are consistent with evolution of suites A and C magmas by fractional crystallization from intermediate compositions towards SiO_2-rich ones. Suite B has low MgO and CaO abundances (<1.1 and <3.0 wt.% respectively), but its low-SiO_2 samples plot on the same MgO–SiO_2 and CaO–SiO_2 line as suites A and C (Fig. 5a, b). Na_2O and K_2O are positively correlated with higher SiO_2 in suites A and C, although Suite C has the lower Na_2O abundances. In Suite B Na_2O and K_2O have scattered distributions with a distinct negative correlation between Na_2O and SiO_2 in the most silicic rocks (Fig. 5c). TiO_2, Al_2O_3, Fe_2O_3(T), MnO, and P_2O_5 are lower at higher SiO_2 concentrations in all three suites. Suite C has the lowest

https://doi.org/10.1017/S0954102096000260 Published online by Cambridge University Press

Al_2O_3 abundances and lowest aluminium saturation at any silica value (Fig. 5d, e). There is a general trend from metaluminous to peraluminous compositions with higher SiO_2 in the three suites, which is a normal relationship for west Antarctic, Pacific margin, I-type granitoid suites (Leat *et al.* 1993, 1995, Muir *et al.* 1995). Suite A granitoids are metaluminous to peraluminous, with a range of aluminium saturation among the more silicic samples. Suite B granitoids are peraluminous, with weak correlation of aluminium saturation with silica abundance. Suite C granitoids are metaluminous. These relationships are consistent with a greater proportion of magma derived from aluminous crustal rocks of metasedimentary origin in suites A and B than in Suite C.

Selected trace elements are plotted against SiO_2 in Fig. 6. Cr and Ni show a clear negative correlation with SiO_2 in all three suites, and are most abundant (140–200 ppm and 55–62 ppm respectively) in the low-SiO_2 samples of Suite A. V, Zn, Cu and Ga show similar relationships. The distinctive curved trend for Suite A samples in Fig. 6a, with Ni abundances falling rapidly with higher SiO_2 (in the least silicic samples) is similar to the trend for MgO and is consistent with fractional crystallization, rather than magma mixing alone, being the dominant control relating less- to more-silicic samples. The plot of Sr versus SiO_2 distinguishes between the three suites, Suite A granitoids have intermediate Sr compositions for a given value of SiO_2, Suite B granitoids have high values and Suite C low values (Fig. 6b). Rb abundances correlate positively with SiO_2 in all suites, although Suite B has the lowest Rb at any SiO_2 value. None of the samples is markedly rich in Rb; in the Rb versus Y+Nb discrimination diagram (Pearce *et al.* 1984, not shown), most samples plot in the volcanic arc granite field, and a few Suite A samples plot in the low-Rb part of the syn-collision granite field.

The three suites show contrasting behaviour in the Y versus SiO_2 plot (Fig. 6c), and similar relationships are seen in the Th versus SiO_2 plot (not shown). In Suite C, Y abundances increase with increasing SiO_2, plausibly a result of fractional crystallization of a mineral assemblage in which Y is incompatible. In Suite A, Y has a *negative* correlation with SiO_2, a relationship that requires the fractionation of garnet. Because garnet is likely to be an equilibrium phenocryst phase only in strongly peraluminous silicic magmas (Hawkesworth & Clarke 1994), the most probable explanation is that the more silicic (Y-poor) samples of Suite A contain large components of high-Si melts derived by partial melting of garnet-bearing crustal lithologies. Since the silicic, Y-poor samples of Suite A also have low Th abundances ($\leq$6 ppm), the partially melted source probably also contained monazite as a restite phase, and is therefore likely to have been peraluminous (Rapp *et al.* 1987) and metasedimentary. The plots of Zr and Ba versus SiO_2 (Fig. 6d, e) are consistent with evolution of Suite C dominated by fractional crystallization, with zircon and alkali feldspar both becoming significant

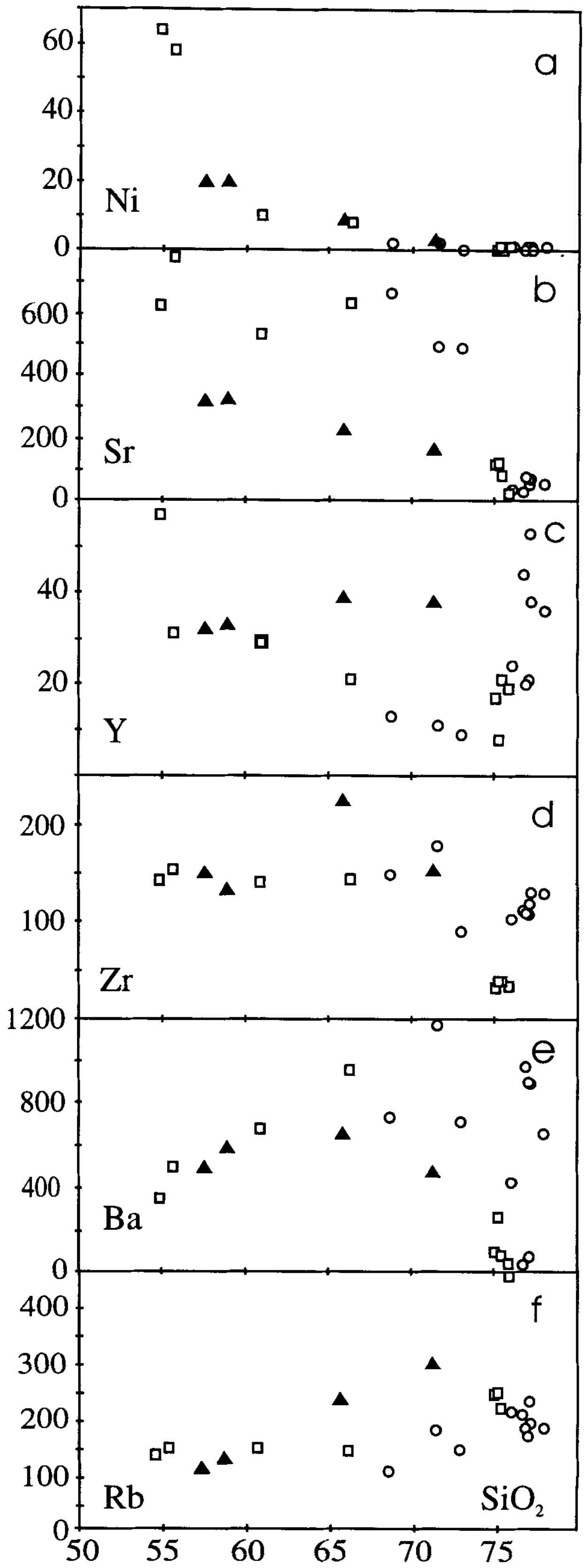

Fig. 6. Harker diagrams for selected trace element whole-rock compositions of the three suites of granitoids, Mount Charity. Symbols as in Fig. 5.

https://doi.org/10.1017/S0954102096000260 Published online by Cambridge University Press

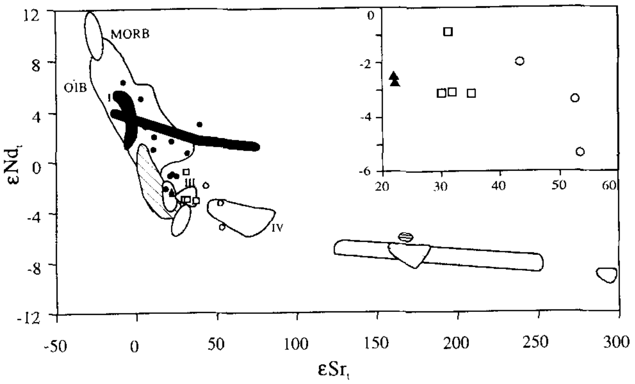

Fig. 7. ϵNd_t versus ϵSr_t diagram showing the composition of Mount Charity samples relative to MORB, OIB, and groups of Antarctic Peninsula intrusive and metamorphic rocks. Errors are within the size of the inset symbols. Dark shading = Late Cretaceous and Tertiary plutonic rocks (Hole *et al.* 1991 and authors' unpublished data), diagonal rule = Early Cretaceous silicic intrusive rocks (Leat *et al.* 1995), light shading = Triassic–Jurassic plutonic rocks of eastern Graham Land and eastern Palmer Land (Hole *et al.* 1991, Wever *et al.* 1994), wavy pattern = gneisses of eastern Graham Land and eastern Palmer Land (Hole *et al.* 1991, Wever *et al.* 1994), horizontal rule = Curran Bluff two-mica granite (Hole *et al.* 1991). The symbols I, III and IV identify groups of granitoids after Hole *et al.* (1991). Symbols for Mount Charity samples in main diagram and inset as in Fig. 5. ● = Cretaceous mafic dykes (authors' unpublished data).

fractionating phases at 65–70 wt.% SiO_2. Suite A shows similar behaviour to Suite C for these elements, implying that fractional crystallization may also have been important in its genesis. Suite B has scattered abundances of Y, Th, Ba and, to some extent, Zr, at any value of SiO_2, inconsistent with fractional crystallization along a single-liquid line of descent. The large range in Y abundances for this suite, at almost constant SiO_2 (Fig. 6c), is consistent both with partial melting of crustal rocks of variable garnet content, and with different degrees of consumption of garnet during a crustal partial melting event.

In summary, the three suites show contrasting elemental relationships. The observed relationships in Suite C probably resulted from fractional crystallization of the sampled phenocryst assemblage from an intermediate magma. The assemblage was dominated by plagioclase. Amphibole, biotite and pyroxene were important ferromagnesian phenocrysts, and their crystallization accounts for the decrease in MgO, Ni and Cr with increasing SiO_2. Concomitant decreases in P and Ti indicate apatite and Fe–Ti oxide fractionation. Zircon and alkali feldspar became significant fractionating phases at 65–70 wt.% SiO_2, when Ba and Zr started to fall with increasing SiO_2. The incompatible behaviour of Y and Th indicate that the assemblage was garnet- and monazite-free. Suite A shows similar patterns to Suite C, indicating, at first sight, that a similar process was responsible for its evolution. Nevertheless, there are significant differences between the groups in that: a) Suite A is more aluminous, being peraluminous in its more silicic compositions, and b) the low Y and Th abundances of Suite A can only be explained satisfactorily if its more silicic members contain a large proportion of peraluminous partial melt of garnet- and monazite-bearing crust. The progressive decrease in Y with increasing SiO_2 in Suite A indicates, moreover, that mixing took place between the intermediate and silicic magmas. Suite A, therefore, is considered to have evolved via mixing of magmas generated from two different sources with similar initial $^{87}Rb/^{86}Sr$, and by fractional crystallization. The more dominant of these processes cannot be established from the present data, but evidence for fractional crystallization is more apparent in the mafic members of the suite and evidence for mixing/hybridization in the silicic members. Suite B has rather limited, silicic, peraluminous compositions that probably were generated by partial melting of crustal sources. Abundances of many major and trace elements are clustered, indicating that the magmas that formed this suite were closely related.

Sm–Nd isotope data

Representative samples from each suite were analysed for Sm and Nd to try to identify the sources of the granitoids. The three Mount Charity plutons have subtly different Sm–Nd isotopic characteristics which broadly mirror the differences in Sr isotopes (Table III and Fig. 7). Values of $^{143}Nd/^{144}Nd_i$ for Suite A are 0.51218–0.51230, for Suite B, 0.51215–0.51232, and for Suite C, 0.51235–0.51236. All three suites have negative ϵNd and positive ϵSr, broadly comparable to other Jurassic and Early Cretaceous granitoids of the Antarctic Peninsula (Fig. 7). In the plot of ϵNd_t vs ϵSr_t, the Mount Charity samples form a small section of a hyperbolic curve between depleted mantle material and enriched crustal material. The relatively small differences in Sr and Nd isotopic compositions of the three suites could have resulted from small differences in the proportions of mantle and crustal contributions to the granitoids (cf. Hole *et al.* 1991), or from generation of the granitoids from isotopically different crustal sources. The mineralogical and compositional differences between the three suites are sufficiently large that we consider tapping of different sources likely.

Relationships to tectonics

Several accounts of Antarctic Peninsula development have emphasized that different episodes of magmatism during the Mesozoic were related to changing tectonic stress regimes (Meneilly *et al.* 1987, Pankhurst *et al.* 1988, Storey *et al.* 1992, 1996, Leat *et al.* 1995). Locally, plutons were intruded along (mostly extensional) faults and shear zones (Storey *et al.* 1996). In particular, studies in north-western Palmer Land have shown that shear zone movements were coeval with plutonism in Early Jurassic and Early Cretaceous times (Vaughan & Millar 1996, A.P.M. Vaughan unpublished data).

There is some evidence that faults may control the ascent of granitoid magma in strike-slip, tensional and compressional regimes (e.g. Hutton & Reavy 1992, Paterson & Fowler 1993, Ingram & Hutton 1994). The close spatial association of plutons of different ages at Mount Charity is consistent with a common, periodically reactivated, magmatic plumbing system. However, in the absence of structural data it is not possible to determine whether the tectonic regimes at the time of emplacement of Mount Charity granitoids were strike-slip, tensional or compressional. Nor is it possible to determine if a single fault system or intersection of more than one fault system controlled magma ascent. However, the structural histories of other parts of the Antarctic Peninsula can be used to provide background control on tectonic regimes coeval with Mount Charity magmatism.

Middle–Late Triassic

The Mount Charity granitoids dated at 232 ± 4 Ma were emplaced synchronously with comparable rocks in eastern Graham Land (Hole *et al.* 1991). In addition, north-western Palmer Land contains deformed gneissose granites that have primary igneous emplacement ages of 220–230 Ma (I.L. Millar, personal communication 1995). The tectonic stress regime at this time is not well understood, but structural examination of megacrystic granite dated at 221 ± 14 Ma from eastern Palmer Land (Storey *et al.* 1996) suggests Late Triassic, east–west extension during magma emplacement. Middle Triassic granitoids from Mount Charity show layered and aligned-feldspar phenocryst fabrics suggesting syn-magmatic simple shear (J.H. Scarrow unpublished data). To the north, Late Triassic to Early Jurassic syn-transtensional magmatism is evident on the Gastre fault system in Patagonia (Rapela & Pankhurst 1992), suggesting widespread arc extension and transtension during the early Mesozoic.

Middle Jurassic

The 168 ± 1 Ma granitoids at Mount Charity are reasonably close, in both age and initial $^{87}Sr/^{86}Sr$, to strongly deformed granitoids at Mount Sullivan, 40 km north–north–east of Mount Charity (178 ± 2 Ma, 0.7075 ± 0.0005, Pankhurst 1983). The plutons are coeval with extensional back-arc sedimentary rocks of the Latady Formation and rhyodacitic to andesitic volcanic rocks of the Mount Poster Formation in south-eastern Palmer Land (Rowley *et al.* 1983). The environment of this basin was probably extensional (Meneilly *et al.* 1987), and terminated in latest Jurassic times (Macdonald & Butterworth 1990), with east–west shortening and east-directed thrusting associated with the Palmer Land deformation event (Kellogg & Rowley 1991, Meneilly *et al.* 1987). Middle Jurassic extension was locally accompanied by dextral shear movements, e.g. on the Auriga Nunataks shear zone; extension continued until at least 188 Ma (A.P.M. Vaughan unpublished data) and may have been active throughout most of the Jurassic.

Early Cretaceous

The final phase of granite magmatism at Mount Charity was part of a large-scale episode of plutonism along the length of the Antarctic Peninsula (Leat *et al.* 1995), that is inferred to have been synchronous with large amounts of east–west extension (Storey *et al.* 1996). East–west extension/dextral transtension occurred on ductile shear zones in north-western Palmer Land (Vaughan & Millar 1996).

Discussion

The three suites of granitoids at Mount Charity have contrasting mineralogical and geochemical features indicating that different sources, or proportions of contributions from sources, were involved in their genesis. The Sr and Nd isotopic characteristics of the suites are broadly similar, but have significant differences (especially in elemental and isotopic Sr contents) which again imply that more than one source was involved. Suite B and the silicic samples of Suite A have S-like compositions and contain a component of partial melting of peraluminous metasedimentary crust, which is the kind of source usually considered most likely for S-type granites (e.g. Chappell & White 1992, Stephens 1992, Pitcher 1993). Suite C and the less silicic sample of Suite A have I-type compositions. There are two plausible models for the origin of these I-type magmas:

a) mantle melting and fractional crystallization with or without crustal contamination, and

b) anatexis of pre-existing igneous rocks.

In view of the limited range of compositions in the Mount Charity samples, it is not possible to be certain about which sources were tapped, although the absence of any mafic, Mg-rich compositions would be consistent with an absence of a voluminous mantle-derived component. I-type granitoids are now commonly regarded as having been derived by partial melting of igneous crust (e.g. Chappell & White 1992, Stephens, 1992, Pitcher 1993). Such a model is supported by experimental evidence that partial melting of tholeiitic basalt will produce tonalitic melts of the composition that commonly forms the more mafic representatives of I-type suites (Clemens & Vielzeuf 1987, Rushmer 1991). If a large proportion of a crustal profile consists of such mafic igneous rock, perhaps underplated in an arc or extending continental margin environment, then the volume of melt generated could be very large. Atherton (1990) proposed that much of the Coastal Batholith of Peru was generated in this way. Leat *et al.* (1995) considered that the Early Cretaceous I-type plutonic

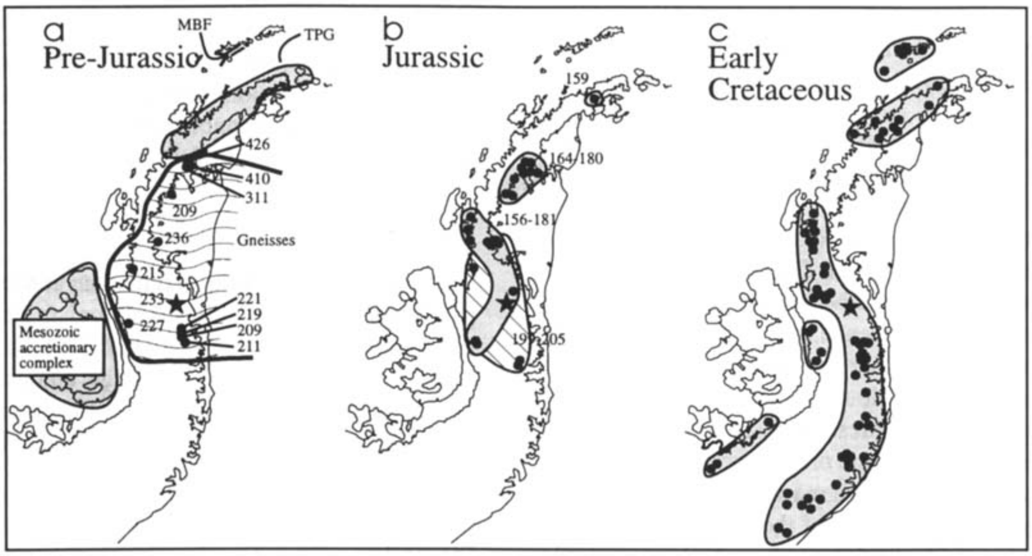

Fig. 8. Sketch maps of the Antarctic Peninsula, showing known extent of plutonism during pre-Jurassic, Jurassic and Early Cretaceous times (after Leat *et al.* 1995). Filled circles indicate radiometric age determinations; the star shows position of Mount Charity. **a.** Pre-Jurassic granitoids. MBF (Miers Bluff Formation) and TPG (Trinity Peninsula Group) are late Palaeozoic to early Mesozoic relatively low-grade metasedimentary rocks (Willan *et al.* 1994, Smellie & Millar 1995); the gneisses in southern Graham Land and northern Palmer Land are generally of much higher grade (indicated ages are either intrusive or metamorphic). **b.** Jurassic intrusions can be divided into earlier (diagonal rule) and later (shaded) episodes (Leat *et al.* 1995). **c.** Early Cretaceous intrusions.

episode in the Antarctic Peninsula, of which Suite C of Mount Charity forms a part, was derived dominantly by partial melting of igneous crust. For these reasons, we consider it more likely that the source of the Mount Charity I-type granitoids was igneous crust.

Partial melting of crust, igneous or sedimentary, normally requires thermal energy to be transported to the site of melting by mantle-derived magmas (Wyllie 1983, Johannes 1983, Huppert & Sparks 1988). It follows that mantle-derived magmas are liable to mix with both I-type and S-type silicic magma generated by crustal partial melting (Hildreth & Moorbath 1988, Grey 1990, Pitcher 1993). Although a direct contribution of mantle-derived magmas to any of the granitoids suites at Mount Charity cannot be proved, their involvement in the magmatism can be inferred from such arguments. In Fig. 7, Late Cretaceous to Early Tertiary dykes scatter between ϵNd_t values of *c.* +6 and -3. This range is thought to represent mantle values beneath the Antarctic Peninsula, high ϵNd values representing asthenosphere and low ϵNd values representing lithospheric mantle (Storey & Alabaster 1991, Scarrow *et al.* 1995). Since the latter are close to the values of the Mount Charity samples, a contribution from lithospheric mantle in the granitic magmas could not easily be identified isotopically.

Figure 8 summarizes the distribution of plutonic activity throughout the Antarctic Peninsula at the times of intrusion of the Mount Charity suites. Mount Charity lies within each zone of known Triassic, Jurassic and Cretaceous plutonism, which overlap in this area. Triassic and Jurassic plutonism was distributed across the width of the arc, but was mostly restricted to the middle latitudes of the Peninsula. In contrast, Early Cretaceous plutonism seems to have been restricted to relatively narrow zones which extended the full length of the Peninsula and which broadened eastward with time (Fig. 8). The change in source characteristics at Mount Charity therefore reflects comparable changes in sources over a large part of the central Antarctic Peninsula. We suggest that tectonic control of magmatic plumbing systems controlled the kind of sources which were tapped during each period (Pankhurst *et al.* 1988). During the Triassic and Jurassic episodes, mafic mantle-derived magma was perhaps able to penetrate to higher levels in the crust, where it caused partial melting of metasedimentary rocks, whilst during the Early Cretaceous episode, mafic magma was ponded at deeper levels, so melting igneous lower crust.

Conclusions

New Rb–Sr whole-rock data for granitoids from Mount Charity, north-eastern Palmer Land identify three phases of plutonism in Middle–Late Triassic (Suite A), Middle Jurassic (Suite B) and Early Cretaceous times (Suite C). Suite A granitoids have both peraluminous (S-like compositions) and metaluminous (broadly I-type compositions) mineralogy. Suite B granitoids have the most peraluminous mineralogy, containing ilmenite and not hornblende, and are S-like. Suite C granitoids have metaluminous mineralogy, containing biotite and hornblende, and are I-type. There is a general trend from metaluminous to peraluminous compositions with increasing SiO_2 within the three suites. The three Mount Charity suites have subtly different Nd isotopic characteristics which broadly mirror more notable differences

https://doi.org/10.1017/S0954102096000260 Published online by Cambridge University Press

in Sr isotopes; all three suites have negative ∈Nd and positive ∈Sr. The mineralogical and compositional differences between the three suites are sufficiently large that we consider it likely that different sources were tapped. Sr and Nd isotopic compositions of the Mount Charity granitoids are intermediate between depleted asthenosphere and high ∈Sr, low ∈Nd crustal compositions from Palmer Land, allowing a wide range of potential sources for the magmas. The data indicate that the S-like magmas contain components of partial melts of garnet-bearing, metasedimentary crust, whereas the I-type magmas probably represent partial melts of meta-igneous crust. A direct lithospheric mantle contribution, by hybridisation with mafic magmas, cannot be proved, but is possible (cf. Storey & Alabaster 1991).

Despite the absence of local structural data, the repeated magmatism at Mount Charity is consistent with a crustal-scale fault or intersection of faults, possibly rooted in the mantle, acting as a preferred ascent pathway for silicic magma as dykes.

Acknowledgements

We are grateful to Chris Wareham for critically reading earlier versions of the manuscript, and to reviewers Malcom Hole and Steve Weaver who gave constructive advice that considerably improved the manuscript. This paper is recorded as NERC Isotope Geosciences Laboratory Publication No. 147, and is a contribution to IGCP Project No. 345 (Andean lithospheric evolution).

References

ATHERTON, M.P. 1990. The Coastal Batholith of Peru: the product of rapid recycling of 'new' crust formed within a rifted continental margin. *Geological Journal*, **25**, 337–349.

BECKINSALE, R.D. 1979. Granite magmatism in the tin belt of South-east Asia. *In* ATHERTON, M.P. & TARNEY, J., *eds. Origin of granite batholiths.* Nantwich, Cheshire: Shiva, 34–44.

CARMICHAEL, I.S.E. & NICHOLLS, J. 1967. Iron-titanium oxides and oxygen fugacities in volcanic rocks. *Journal of Geophysical Research*, **72**, 4665–3687.

CHAPPELL, B.W. & WHITE, A.J.R. 1992. I- and S-type granites of the Lachlan fold belt. *Transactions of the Royal Society of Edinburgh*, Earth Sciences, **83**, 126.

CLEMENS, J.D. & VIELZEUF, D. 1987. Constraints on melting and magma production in the crust. *Earth and Planetary Science Letters*, **86**, 287–306

CZAMNSKE, G.K., ISHIHARA, S. & ATKIN, S.A. 1981. Chemistry of rock forming minerals of the Cretaceous–Paleocene batholith in south-western Japan and implications for magma genesis. *Journal of Geophysical Research*, **86**, 10431–10469.

DAVIES, T.G. 1971. The geology of Mount Charity, the eastern side of mounts Hope and Faith, and eastwards through Mount Sullivan to Engel Peaks. *British Antarctic Survey Interim Report*, No. G5/1971/E[Unpublished].

DAVIES, T.G. 1984. The geology of part of northern Palmer Land. *British Antarctic Survey Scientific Reports*, No. 103, 46 pp.

FLOYD, P.A. 1985. Petrology and geochemistry of oceanic intra-plate sheet flow basalts, Naruru Basin, Deep Sea Drilling Project leg 89. *In* MOBERLY, R., SCHLANGER, S.O. *et al., eds. Initial Reports of the Deep Sea Drilling Project*, **89**, 471–497.

GREY, C.M. 1990. A strontium isotopic traverse across the granitic rocks of south-eastern Australia: petrogenetic and tectonic implications. *Australian Journal of Earth Sciences*, **37**, 331–349.

HAWKESWORTH, C. & CLARKE, C. 1994. Partial melting in the lower crust: new constraints on crustal contamination processes in the central Andes. *In* REUTTER, K.-J., SCHEUBER, E. & WIGGER, P.J., *eds. Tectonics of the central Andes.* Berlin: Springer-Verlag, 93–101.

HILDRETH, W. & MOORBATH, S. 1988. Crustal contributions to arc magmatism in the Andes of central Chile. *Contributions to Mineralogy and Petrology*, **98**, 455–489.

HOLE, M.J., PANKHURST, R.J. & SAUNDERS, A.D. 1991. Geochemical evolution of the Antarctic Peninsula magmatic arc: the importance of mantle–crust interactions during granitoid genesis. *In* THOMSON, M.R.A., CRAME, J.A. & THOMSON, J.W., *eds. Geological evolution of Antarctica.* Cambridge: Cambridge University Press, 369–374.

HUPPERT, H.E. & SPARKS, R.S.J. 1988. The generation of granitic magmas by intrusion of mafic magmas into the crust. *Journal of Petrology*, **29**, 599–624.

HUTTON, D.H.W. & REAVY, R.J. 1992. Strike-slip tectonics and granite petrogenesis. *Tectonics*, **11**, 960–967.

INGRAM, G.M. & HUTTON, D.H.W. 1994. The Great Tonalite Sill: emplacement into a contractional shear zone and implications for Late Cretaceous to early Eocene tectonics in south-eastern Alaska and British Columbia. *Geological Society of America Bulletin*, **106**, 715–728.

JOHANNES, W. 1983. Metastable melting in granite and related systems. *In* ATHERTON, M.P. & GRIBBLE, C.D., *eds. Migmatites, melting and metamorphism.* Nantwich, Cheshire: Shiva, 27–36.

KELLOGG, K. & ROWLEY, P.D. 1991. Tectonic evolution of the south-eastern Antarctic Peninsula. *In* THOMSON, M.R.A., CRAME, J.A. & THOMSON, J.W., *eds. Geological evolution of Antarctica.* Cambridge: Cambridge University Press, 461–465.

LEAT, P.T., SCARROW, J.H. & MILLAR, I.L. 1995. On the Antarctic Peninsula batholith. *Geological Magazine*, **132**, 399–412.

LEAT, P.T., STOREY, B.C. & PANKHURST, R.J. 1993. Geochemistry of Palaeozoic–Mesozoic Pacific rim orogenic magmatism, Thurston Island area, West Antarctica. *Antarctic Science*, **5**, 281–296.

MACDONALD, D.I.M. & BUTTERWORTH, P.J. 1990. The stratigraphy, setting and hydrocarbon potential of the Mesozoic sedimentary basins of the Antarctic Peninsula. *In* ST. JOHN, B., *ed. Antarctica as an exploration frontier.* American Association of Petroleum Geologists, Studies in Geology, No. 31, 102–125.

MENEILLY, A.W., HARRISON, S.M., PIERCY, B.A. & STOREY, B.C. 1987. Structural evolution of the magmatic arc in northern Palmer Land, Antarctic Peninsula. *In* MCKENZIE, G.D., *ed. Gondwana six: structure, tectonics and geophysics.* American Geophysical Union, Geophysical Monograph, No. 40, 209–219.

MOYES, A.B. 1991. Variations in amphibole compositions from the Andean intrusive suite across the Antarctic Peninsula. *In* THOMSON, M.R.A., CRAME, J.A. & THOMSON, J.W., *eds. Geological evolution of Antarctica.* Cambridge: Cambridge University Press, 375–379.

MUIR, R.J., WEAVER, S.D., BRADSHAW, J.D. EBY, G.N. & EVANS, J.A. 1995. The Cretaceous Separation Point batholith, New Zealand: granitoid magmas formed by melting of mafic lithosphere. *Journal of the Geological Society of London*, **152**, 689–701.

PANKHURST, R.J. 1981. Preliminary geological report, north-eastern Palmer Land, 1980–81. *British Antarctic Survey Interim Report*, No. G3/1980-81/R [Unpublished].

PANKHURST, R.J. 1982. Rb–Sr geochronology of Graham Land, Antarctica. *Journal of the Geological Society of London*, **139**, 701–711.

PANKHURST, R.J. 1983. Rb–Sr constraints on the ages of basement rocks of the Antarctic Peninsula. *In* OLIVER, R.L., JAMES, P.R. & JAGO, J.B., *eds. Antarctic earth science.* Canberra: Australian Academy of Science &

Cambridge: Cambridge University Press, 367–371.

Pankhurst, R.J. 1990. The Paleozoic and Andean magmatic arcs of West Antarctica and southern South America. *Geological Society of America Special Paper*, No. 241, 17.

Pankhurst, R.J. & Rowley, P.D. 1991. Rb–Sr study of Cretaceous plutons from southern Antarctic Peninsula and eastern Ellsworth Land, Antarctica. *In* Thomson, M.R.A., Crame, J.A. & Thomson, J.W., *eds. Geological evolution of Antarctica*. Cambridge: Cambridge University Press, 387–394.

Pankhurst, R.J., Hole, M.J. & Brook, M. 1988. Isotope evidence for the origin of Andean granites. *Transactions of the Royal Society of Edinburgh*, Earth Sciences, **79**, 123–133.

Paterson, S.R. & Fowler, T.K., Jr. 1993. Extensional pluton-emplacement models: do they work for large plutonic complexes? *Geology*, **21**, 781–784.

Pearce, J.A., Harris, N.B.W. & Tindle, A.G. 1984. Trace element discrimination diagrams for the tectonic interpretation of granitic rocks. *Journal of Petrology*, **25**, 956–983.

Pitcher, W.S. 1993. *The nature and origin of granite*. London: Blackie, 321 pp.

Rapela, C.W. & Pankhurst, R.J. 1992. The granites of northern Patagonia and the Gastre Fault System in relation to the break-up of Gondwana. *In* Storey, B.C., Alabaster, T. & Pankhurst, R.J., *eds. Magmatism and the causes of continental break-up*. Special Publication of the Geological Society, London, No. 68, 209–220.

Rapp, R.P., Ryerson, F.J. & Miller, C.F. 1987. Experimental evidence bearing on the stability of monazite during crustal anatexis. *Geophysical Research Letters*, **14**, 307–310.

Rex, D.C. 1976. Geochronology in relation to the stratigraphy of the Antarctic Peninsula. *British Antarctic Survey Bulletin*, No. 43, 49–58.

Rowley, P.D., Vennum, W.R., Kellogg, K.S., Laudon, T.S., Carrara, P.E., Boyles, J.M. & Thomson, M.R.A. 1983. Geology and plate tectonic setting of the Orville Coast and eastern Ellsworth Land, Antarctica. *In* Oliver, R.L., James, P.R. & Jago, J.B., *eds. Antarctic earth science*. Canberra: Australian Academy of Science & Cambridge: Cambridge University Press, 245–250.

Rushmer, T. 1991. Partial melting of two amphibolites: contrasting experimental results under fluid-absent conditions. *Contributions to Mineralogy and Petrology*, **107**, 41–59.

Saunders, A.D. & Tarney, J. 1982. Igneous activity in the southern Andes and northern Antarctic Peninsula: a review. *Journal of the Geological Society of London*, **139**, 691–700.

Saunders, A.D., Tarney, J. & Weaver, S.D. 1980. Transverse geochemical variations across the Antarctic Peninsula: implications for the genesis of calc-alkaline magmas. *Earth and Planetary Science Letters*, **46**, 344–360.

Scarrow, J.H., Leat, P.T., Millar, I.L., Wareham, C.D., & Griffiths, C.G. 1995. Antarctic Peninsula magmatism: mantle and crustal sources. *Mineralogical Society Bulletin*, No. 107, 14.

Simpson, C. & Wintsch, R.P. 1989. Evidence for deformation-induced K-feldspar replacement by myrmekite. *Journal of Metamorphic Geology*, **7**, 261–275.

Smellie, J.L. & Millar, I.L. 1995. New K–Ar isotopic ages of schists from Nordenskjöld Coast, Antarctic Peninsula: oldest part of the Trinity Peninsula Group? *Antarctic Science*, **7**, 191–196.

Stephens, W.E. 1992. Spatial, compositional and rheological constraints on the origin of zoning in the Criffell pluton, Scotland. *Transactions of the Royal Society of Edinburgh:* Earth Sciences, **83**, 191–199.

Storey, B.C. & Alabaster, T. 1991. Tectonomagmatic controls on Gondwana break-up models: evidence from the proto-Pacific margin of Antarctica. *Tectonics*, **10**, 1274–1288.

Storey, B.C., Alabaster, T., Hole, M.J., Pankhurst, R.J. & Wever, H.E. 1992. Role of subduction-plate boundary forces during the initial stages of Gondwana break-up: evidence from the proto-Pacific margin of Antarctica. *In* Storey, B.C., Alabaster, T. & Pankhurst, R.J., *eds. Magmatism and the causes of continental break-up*. Special Publication of the Geological Society, London, No. 68, 149–163.

Storey, B.C., Vaughan, A.P.M. & Millar, I.L. 1996. Geodynamic evolution of the Antarctic Peninsula during Mesozoic times and its bearing on Weddell Sea history. *In* Storey, B.C., King, E.C. & Livermore, R.A., *eds. Weddell Sea tectonics and Gondwana break-up*. Special Publication of the Geological Society, London (in press).

Suárez, M. 1976. Plate-tectonic model for southern Antarctic Peninsula and its relation to southern Andes. *Geology*, **4**, 211–214.

Vaughan, A.P.M. & Millar, I.L. 1996. Early Cretaceous magmatism during extensional deformation within the Antarctic Peninsula magmatic arc. *South American Journal of Earth Sciences* (in press).

Wever, H.E., Millar, I.L. & Pankhurst, R.J. 1994. Geochronology and radiogenic isotope geology of Mesozoic rocks from eastern Palmer Land, Antarctic Peninsula: crustal anatexis in arc-related granitoid genesis. *Journal of South American Earth Sciences*, **7**, 69–83.

Wever, H.E. Storey, B.C. & Leat, P. 1995. Peraluminous granites in NE Palmer Land, Antarctic Peninsula: early Mesozoic crustal melting in a magmatic arc. *Journal of the Geological Society, London*, **152**, 85–96.

Willan, R.C.R., Pankhurst, R.J. & Hervé, F. 1994. A probable Early Triassic age for the Miers Bluff Formation, Livingston Island, South Shetland Islands. *Antarctic Science*, **6**, 401–408.

Wyllie, P.J. 1983. Experimental and thermal constraints on the deep seated parentage of some granitoid magmas at subduction zones. *In* Atherton, M.P. & Gribble, C., *eds. Migmatites, melting and metamorphism*. Nantwich, Cheshire: Shiva, 37–51.